On Advances in Asymmetrical Flow Field Flow Fractionation for Biosample Characterization

Bolinsson, Hans

2024

Document Version:
Publisher's PDF, also known as Version of record

On Advances in Asymmetrical Flow Field Flow Fractionation for Biosample Characterization

HANS BOLINSSON
DEPARTMENT OF PROCESS AND LIFE SCIENCE ENGINEERING | LUND UNIVERSITY

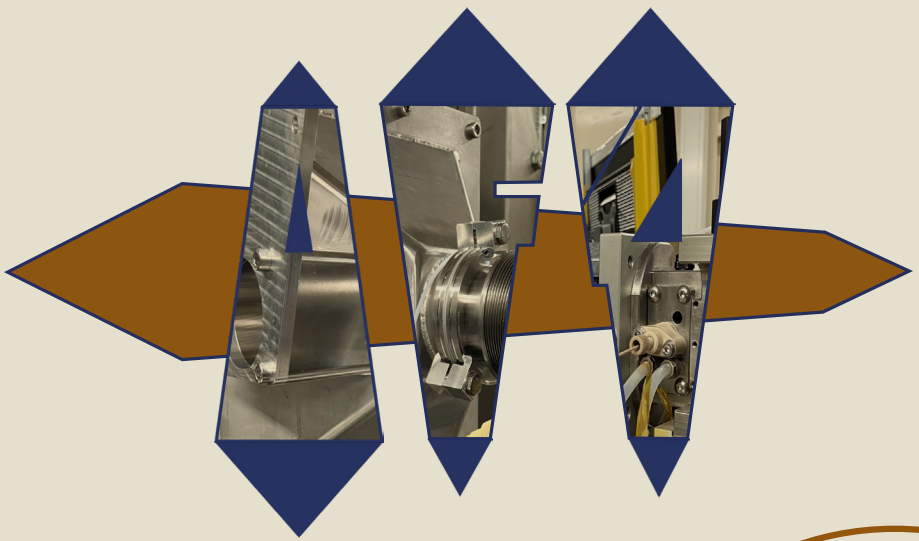

On Advances in Asymmetrical Flow Field Flow Fractionation for Biosample Characterization

Hans Bolinsson

LUND
UNIVERSITY

Department of Process and Life Science Engineering

Faculty of Engineering

Lund University, Sweden

LICENTIATE DISSERTATION

Licentiate dissertation for the degree of Licentiate in Engineering at the Faculty of Engineering, Lund University, to be publicly defended on June 11, 2024, at 13.15 in KC:A, Kemicentrum, Naturvetarvägen 14, Lund, Sweden

Faculty opponent
Dr. Per-Olof Wahlund, Novo Nordisk

Organization: LUND UNIVERSITY

Document name: Licentiate Thesis **Date of issue: 2024-05-27**

Author(s): Hans Bolinsson **Sponsoring organization:VINNOVA**

Title and subtitle: On Advances in Asymmetrical Flow Field Flow Fractionation for Biosample Charaterization

Abstract:

Asymmetrical Flow Field Flow Fractionation is a technique with high versatility and is used for size fractionation of polydisperse and widely size distributed samples from various fields of research. Colloidal samples in food systems, formulated biologics from pharmaceutical science, nanoparticles from water treatment systems, molecular distributions in extracted material from wood science, and lipid nano-particles for vaccine production are a few applications where measurements can, have and will help researchers to gain better understanding and knowledge of a sample under investigation. In this thesis, two advances in the utilization of AF4, which is the abbreviation for the technique, are presented. These advances can be applied in any of the above mentioned examples. The first paper suggests a novel and more robust calibration methodology for the height of the fractionation channel. The height of the channel is determined to be able to calculate the hydrodynamic size of analytes. The second paper is also a method paper, and a proof-of-concept paper for the direct or on-line coupling between the AF4 channel and the flow-through capillary of synchrotron BioSAXS. The utilization of synchrotron X-rays of high flux was considered necessary for the continuous collection of X-ray scattering from dilute, weakly sattering biologics in constant flow or motion.

Key words: AF4, SAXS, biologics, characterization, calibration

Language: English

ISBN (print): 978-91-8096-054-0

ISBN (e-version): 978-91-8096-055-7

Number of pages: 55

Signature Date 2024-05-27

On Advances in Asymmetrical Flow Field Flow Fractionation for Biosample Characterization

Hans Bolinsson

LUND
UNIVERSITY

Faculty of Engineering
Department of Process and Life Science Engineering
Division of Food and Pharma

ISBN(print): 978-91-8096-054-0
ISBN(e-version): 978-91-8096-055-7

Printed in Sweden by Media-Tryck, Lund University
Lund 2024

A person who never made a mistake never tried anything new
Albert Einstein

Table of Contents

Abstract

Asymmetrical Flow Field Flow Fractionation is a technique with high versatility and is used for size fractionation of polydisperse and widely size distributed samples from various fields of research. Colloidal samples in food systems, formulated biologics from pharmaceutical science, nanoparticles from water treatment systems, molecular distributions in extracted material from wood science, and lipid nanoparticles for vaccine production are a few applications where measurements can, have and will help researchers to gain better understanding and knowledge of a sample under investigation. In this thesis, two advances in the utilization of AF4, which is the abbreviation for the technique, are presented. These advances can be applied in any of the above mentioned examples. The first paper in this thesis suggests a novel and more robust calibration methodology for the height of the fractionation channel. The height of the channel is determined to be able to calculate the hydrodynamic size of analytes. The second paper is also a method paper, and a proof-of-concept paper for the direct or on-line coupling between the AF4 channel and the flow-through capillary of synchrotron BioSAXS. The utilization of synchrotron X-rays of high flux was considered necessary for the continuous collection of X-ray scattering from dilute, weakly sattering biologics in constant flow or motion.

Populärvetenskaplig sammanfattning

Denna avhandling sammanfattar två vetenskapliga artiklar som beskriver utvecklingen av nya metoder för användning av fraktioneringstekniken Asymmetrisk Flödesfältsfraktionering eller på engelska Asymmetric Flow Field Flow Fractionation, förkortat AF4. AF4 används för att fraktionera/separera molekyler eller partiklar i en lösning med hjälp av vätskeflöden i en öppen kanal. Flödena utgör både separationsfält och bärarvätska. Separationsfältet eller tvärflödet bromsar olika stora molekyler selektivt, samtidigt som bärarvätskan för provet framåt genom separationskanalen. Vad som är unikt med metoden är att separationskanalen inte innefattar någon stationär fas som växelverkar med innehållet i provet, utan baseras istället i normalfallet på molekylers spontana rörelse, även kallat diffusion eller Brownsk rörelse. AF4 är alltså en storleksbaserad fraktioneringsteknik eftersom den Brownska rörelsen är storleksberoende. Det faktum att separationen utförs i en öppen kanal innebär att den skjuvkraft som molekyler utsätts för är relativt låg. En annan konsekvens av den öppna kanalen är att den yta som molekyler kan växelverka med under själva separationen är relativt liten. Detta tillsammans främjar separation av känsliga och komplexa prover, prover som vid höga skjuvkrafter eller med stor benägenhet att växelverka med ytor annars skulle kunna förstöras eller förändras p.g.a. mätteknikens utformning. Andra främjande egenskaper som gör att det finns anledning att utnyttja tekniken är att valet av bärarvätska görs utifrån provets egenskaper snarare än efter instrumentets krav. Dessutom kan man separera över ett brett storleksområde (från smått till stort) i en och samma mätning.

Detta arbete har delvis finansierats av VINNOVA genom NextBioForm, ett konsortium mellan akademi och industri, som verkar för att utveckla nya metoder för karaktärisering av biologiska läkemedels tillstånd i formulering. Detta för att öka kunskapen om mekanismer som styr stabiliserande och destabiliserande faktorer i läkemedel.

Genom bättre kunskap om stabiliserande faktorer kan formuleringar förhoppningsvis utvecklas, som i det långa loppet främjar patientvänligheten och minskar energiförbrukningen i form av t.ex. lagringstemperatur. Många biologiska läkemedel kräver idag lagring och transport vid -80^{o}C, något som inte går att åstadkomma i varje hem. I samband med Covid-19 pandemin nämndes den så viktiga obrutna kylkedjan som ett problem för snabb och effektiv distribution av vaccinet över världen. Viljan finns att utveckla formuleringar som innebär att den

enskilde patienten ska kunna lagra sitt läkemedel hemma i kylen och administrera själv utan hjälp av specialist på vårdinrättning.

Arbetet med att utveckla nya formuleringar av läkemedel innefattar karaktärisering av de ingående aktiva substanserna och då är storleksmätning ett effektivt sätt att verifiera en substans tillstånd och därmed förmåga att utföra sin tilltänkta uppgift i kroppen. AF4 är en teknik som kan användas för detta, genom att koppla detektorer i serie till separationskanalen kan provet analyseras storleksseparerat och separat över dess beståndsdelar.

En ny metod som verifierats i denna avhandling är kopplingen mellan AF4 och SAXS, applicerat på biologiska molekyler. SAXS är en förkortning för lågvinkel-röntgenspridning, en tillgänglig mätmetod på elektronacceleratorn MAX IV och som bl.a. används för studier av molekyler i lösning. Den korta våglängden i röntgenstrålning gör det möjligt att studera små detaljer, i samma storleksordning som våglängden själv, dvs ner till ca 1 nm (10^{-9} m).

En typ av biologiska läkemedel som det forskas på idag är antikroppar, med potential för t.ex. cancerbehandling. Antikroppen Trastuzumab, som används vid bröstcancerbehandling, har karaktäriserats i en av artiklarna i denna avhandling. Diametern hos en antikropp är i storleksordningen 10 nm och med hjälp av röntgenljus kan storlek, form och struktur granskas. Det är banbrytande resultat som presenteras här. I och med implementeringen av AF4-SAXS som metod för biologiska molekyler går det att studera effekter av olika formuleringar och steg i tillverkningsprocessen, eftersom biologiska läkemedels tillstånd kan studeras in-situ; läkemedlet kan storleksseparera i dess tilltänkta miljö (formulering). Detta minskar risken för påverkan på analysresultatet från avvikelser i formuleringen. Är det rimligt att ta bort en komponent i formuleringen för mätmetodens skull?

Biologiska läkemedels (proteiners) stabilitet är en konsekvens av den miljö de befinner sig i. Ändringar av pH, jonstyrka eller temperatur kan inducera aggregering och/eller denaturering. Dessutom, för att stabilisera biologiska läkemedel, används ofta tillsatser i dess formuleringar, så som konserveringsmedel och ytaktiva (stabiliserande) ämnen. Att kunna göra en storlekbestämning i den slutgiltiga formuleringen ökar tilltron till en framgångsrik formulering.

Det är såklart också en styrka att kunna separera formuleringar med minsta möjliga påverkan i form av skjuvkrafter och ytinteraktioner, båda kan vid godtyckliga omständigheter förändra storlek, form och struktur hos proteiner.

Denna avhandling innehåller också en beskrivning av en ny kalibreringsmetod för AF4.

Storleken på en molekyl kan anges på flera olika sätt och med AF4 kan man i en och samma mätning och med rätt detektorer bestämma molekylvikter och olika storleksangivelser av provet. Ett vanligt förekommande sätt att ange storlek på molekyler är den hydrodynamiska storleken, som beskriver hur en perfekt sfär via

spontan rörelse (diffusion, Brownsk rörelse) rör sig i en vätska. En molekyl som inte är sfärisk, utan istället förgrenad och spretig, kan också definieras med en hydrodynamisk storlek. Denna storleksangivelse anger då motsvarande storlek på en sfär med identiskt hydrodynamiskt beteende som den undersökta molekylen.

Den hydrodynamiska storleken kan bestämmas med hjälp av AF4. I den teori som beskriver sambandet mellan provets uppehållstid i kanalen och storleken, avses den hydrodynamiska storleken. För att kunna beräkna den hydrodynamiska storleken krävs dock en kalibrering av kanalens höjd. Detta har traditionellt gjorts genom att mäta uppehållstiden för ett prov med känd storlek, men i denna avhandling beskrivs ett nytt tillvägagångssätt som använder sig av en nano-emulsion (flera storlekar i samma prov) för en mer robust kalibrering. Nano-emulsionen är stabil i ett pH-område bredare än de prov som normalt sätt använts för kalibrering (protein och standardpartiklar vid neutrala pH) och är dessutom mer kostnadseffektiv. Kalibrering i ett bredare pH-område kan visa sig användbart tex för storleksbestämningar av läkemedel som administreras via mag-tarmkanalen.

List of Papers

Paper I

Bolinsson, H., Lu, Y., Hall, S., Nilsson, L., Håkansson, A.

An alternative method for calibration of flow field flow fractionation channels for hydrodynamic radius determination: The nanoemulsion method (featuring multi angle light scattering),

Journal of Chromatography A, **Volume 1533**, 2018, Pages 155-163, ISSN 0021-9673, https://doi.org/10.1016/j.chroma.2017.12.026.

Paper II

Bolinsson, H., Söderberg, C., Herranz-Trillo, F., Wahlgren, M., Nilsson, L.

Realizing the AF4-UV-SAXS on-line coupling on protein and antibodies using high flux synchrotron radiation at the CoSAXS beamline, MAX IV.

Analytical and Bioanalytical Chemistry, **415**, 6237–6246 (2023). https://doi.org/10.1007/s00216-023-04900-7

Author's contribution to the papers

Paper I

H. B. prepared the samples, performed the AF4 method development, AF4 measurements and analysis and was the main author of the manuscript.

Paper II

H. B. prepared the samples, performed the AF4 method development, AF4-SAXS measurements, AF4 and SAXS analysis and was the main author of the manuscript.

Abbreviations

AF4	Asymmetrical Flow Field Flow Fractionation
AF4-UV-SAXS	Asymmetrical Flow Field Flow Fractionation in on-line coupling to Ultraviolet and Small Angle X-ray Scattering
SAXS	Small Angle X-ray Scattering
XCT	X-ray Computed Tomography
MALS	Multi Angle Light Scattering
SEC	Size Exclusion Chromatography
SEC-SAXS	Size Exclusion Chromatography in on-line coupling to Small Angle X-ray Scattering
HPLC	High Performance Liquid Chromatography
PES	Polyether Sulphone
RC	Regenerated Cellulose
PEEK	Polyether Ether Ketone
DLS	Dynamic Light Scattering
AUC	Analytical Ultracentrifugation
PSD	Particle Size Distribution
BioSAXS	SAXS on biomolecules
P(r)	Pair Distribution Function
UV	Ultraviolet
BSA	Bovine Serum Albumin
SAS	Small Angle Scattering
SANS	Small Angle Neutron Scattering
LNP	Lipid Nano Particle
API	Active Pharmaceutical Ingredient

m-RNA	Messenger-Ribonucleic Acid
LC	Liquid Chromatography
RI	Refractive Index
S/N	Signal to Noise Ratio

Introduction

Particle size fractionation techniques have been used analytically and in production settings for centuries (1). Size fractionation and specifically the analytical approach has become a necessity for the individualized characterization of sizes within polydisperse systems in the sub-micron size range by e.g. static light scattering, where average results otherwise would be the outcome.

Asymmetrical Flow Field Flow Fractionation (AF4) was pioneered by Professor Karl-Gustav Wahlund and co-workers at the Faculty of Engineering, Lund University. In their early papers the strength and possibilities of the methodology was demonstrated by showing high-speed high-resolution fractionations of protein monomer and dimer (2, 3), and monoclonal antibodies (4), as well as crucial development steps, such as the asymmetrical design (5), the downstream sample injection (3) and trapezoidal geometry (6) which lay the foundation for establishing and commercializing the technique. In the coming chapters, AF4 and its usage will be introduced, compared to similar size fractionation techniques, and described in detail for thesis-specific areas of use.

This thesis takes off long after the commercialization of AF4. The use of AF4 is today widely spread over the world and in various research fields (7-13), but as for any other well-established technique there is untrodden ground. With the development history of AF4 at this university, it is a great pleasure to present new advances from Lund University in the usage of the technique (14, 15).

In the development of biopharmaceuticals or biologics (proteins, hormones, antibodies) the research and development tasks before clinical studies deal with formulation. The final formulation should possess properties like long term stability, with patient ease of use and sustainability in mind, ambient storage temperatures are desired. At the same time the active pharmaceutical ingredient (API) needs to be intact and active, avoiding any risk of inducing harmful reactions *in vivo* whether inhaled, injected or orally delivered. For steps in the downstream processing and when evaluating the addition or changes of excipients in drug formulation, size characterization is a powerful tool to establish the state of biologic pharmaceuticals. In cases where the API is prone to aggregate, AF4 is a valuable technique for size fractionation prior to size determination and to establish volume fractions of native and aggregated parts. This is due to AF4's undisputed ability to separate sensitive, large, and widely size-distributed samples, in single runs.

The advancements in the usage of AF4 are in this thesis represented by two scientific publications concerning the calibration of AF4 channels and the direct on-line coupling between AF4 and Small Angle X-ray Scattering (SAXS) (14, 15).

The work has been supported by VINNOVA through the NextBioForm consortium, an industry and academia joint venture for development of new characterization methods to study stability/instability mechanisms for biologics in dry and liquid formulation. This thesis contributes to liquid formulation characterization by paper II, where AF4 was for the first time coupled on-line to SAXS for biomolecule characterization in solution.

The coupling between AF4 and various detectors is standard procedure and very much like in size exclusion chromatography (SEC) or high-performance liquid chromatography (HPLC) the separation device is normally connected in series to size and/or concentration detectors like multi-angle light scattering (MALS), and ultraviolet (UV) or refractive index (RI) detection. Coupling of the AF4 channel to SAXS enables size detection down to 1 nm and opens the door to direct shape and structural information from the size fractionated analytes eluting from the AF4 channel. Biomolecules are low electron density samples and at the same time the fractionation in AF4 dilutes the sample. To achieve adequate SAXS data on proteins eluting from the AF4 channel it was coupled directly to the flow through capillary of the beamline CoSAXS (16) at the synchrotron at MAX IV Laboratory. The high X-ray flux supplied from a synchrotron was considered a must for low electron density samples fractionated by AF4. Combining AF4 with SAXS opens for possibilities to characterize samples alternatively and further, samples with wide and large size distributions as well as for samples of sensitive nature, like casein micelles, liposomes, aggregates, and polymers. The on-line AF4-SAXS is aimed for sample cases where separation is a must, or in other words, where batch measurements in SAXS is not an option. Measuring multiple sizes simultaneously in SAXS batch mode gives a sum-weighted result in the scattering pattern and conclusions may be difficult to draw.

The calibration of the AF4 channel is performed to determine the height of the fractionation channel. With a calibrated channel height, it is possible to determine hydrodynamic radii of analytes by measuring their retention time in the separation device. The calibration advancement presented here utilizes a nano-emulsion with a size distribution, instead of the traditionally used one-particle-size calibration. In a one-particle calibration a sample of known hydrodynamic size is used. The calibration is set to become more robust when calibration is performed using several analyte sizes instead of just one. The idea for the paper comes from the critical review paper by Wahlund (17), where it is suggested to check the validity of the calibration by "using a range of different retention times and to check if channel height is consistent".

Aims/Objectives and Hypothesis

For paper I the aim was to implement a more robust calibration methodology for AF4 channels using one sample with a wide size distribution. The standard way of calibration uses a one particle size method, and a validation using other sizes has been recommended as a complementary thing to do. The new calibration method should be more cost effective and allow for calibrations in a wider pH range compared to calibrations using proteins or standard particles.

Paper I was performed under the hypothesis that a nano-emulsion could be used for the purpose of calibrating an AF4 channel with several sizes in one measurement.

A nano-emulsion can be created using standard chemical laboratory equipment, which makes it cost effective. A nano-emulsion can also have a maintained stability in a wider pH range compared to proteins and standard particles, depending on the surfactant used.

For paper II the aim was to perform a proof-of-concept of the AF4-UV-SAXS on-line coupling on biomolecules/proteins by collection of adequate S/N on-line SAXS data, following AF4 fractionation.

This was performed under the hypothesis that the high X-ray flux supplied at CoSAXS beamline would be sufficient for on-line SAXS data collection from fractionated protein and antibody assemblies.

Asymmetrical flow field flow fractionation (AF4)

AF4 is a technique used for the fractionation of colloidal samples or large molecules in solution, whether its polymers, biomolecules, nanoparticles, or casein micelles, they can be size fractionated based on their hydrodynamic size. The most common way of AF4 operation is in Brownian mode where sizes between a few nanometers up to about 1 micron can be fractionated (2-1000 nm). For larger sizes hyperlayer- and steric effects interfere with diffusion-based separation (18). The hydrodynamic size is related to the diffusion coefficient (Brownian motion) and defined as the equivalent size of a sphere having the same hydrodynamic behavior as the molecule/particle under investigation. The fractionation works under the principle of two opposing forces, or transport phenomena, acting on the analytes. A schematic overview is presented in figure 1 (19). Diffusional transport is acting in the opposite direction to the crossflow-induced transport. At a set crossflow, diffusional transport will be the selective quantity between analytes.

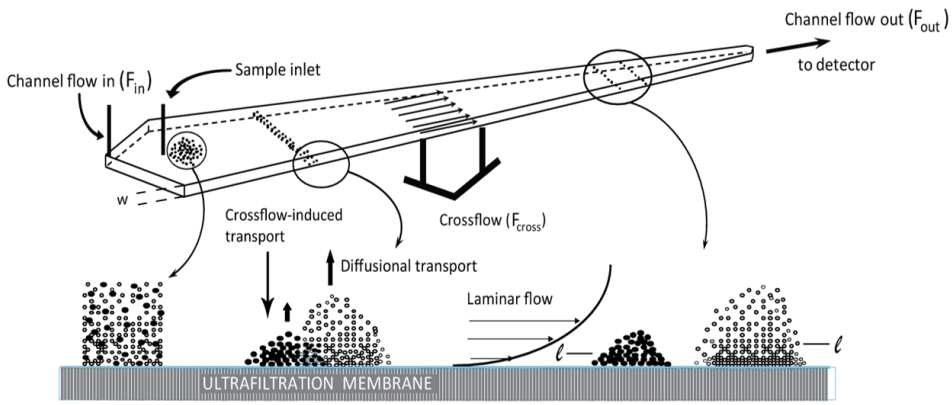

Fig. 1. Schematic view of an AF4 fractionation and channel geometry (19). Reproduced with permission from Springer.

When the size of analytes increases, the diffusional transport as a selective quantity can be set out of play. Steric elution or reversed order elution happens when the analyte is physically too large (the diffusion coefficient decreases with size) and is pressed against the accumulation wall by the crossflow, while experiencing a higher elution flow than what the relaxed height position in Brownian mode would allow. The other effect which can occur for large analyte sizes is the hyperlayer effect, which is caused by a buoyancy force acting on the analyte due to carrier flow inertia. The resulting effect is an elevated layer, hyperlayer, of focused sample away from their expected average distance from the accumulation wall.

The steric/hyperlayer effect results in coelution of sizes when in combination with Brownian mode and the results are difficult to interpret. The vast majority of fractionations in AF4 are performed in Brownian mode and for the user it is of great importance to be aware of reversed order effects when interpreting results.

The fractionation is performed in a channel, which is geometrically defined by a spacer with a punched geometry in it. In the commercially available instruments this punched geometry has the shape of a trapezoid. The spacer is clamped between two solid blocks to define the upper and the lower confinements of the channel. In the bottom of the channel sits a frit, normally made from stainless steel, and on top of that an ultrafiltration membrane, which is then supported by the frit (figure 2). The purpose of the frit and the membrane is to let carrier liquid escape from the channel. This escaping flow is named crossflow, and is the ground for crossflow-induced transport, forcing the analytes towards the ultrafiltration membrane. The ultrafiltration membrane has an appropriate cutoff for the application and should be chosen to prevent analytes from leaving the channel through the membrane. A typical cutoff is 10 kDa and frequently used materials are regenerated cellulose (RC), and polyether sulfone (PES).

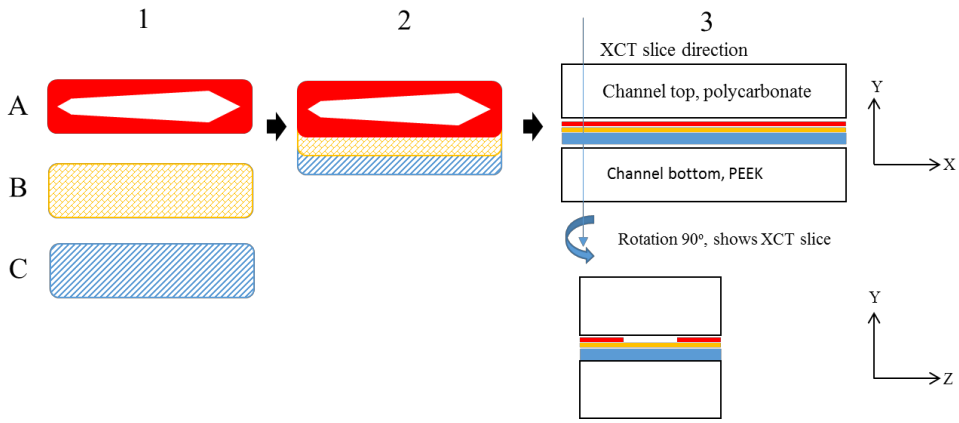

Fig. 2. Schematic illustration of the AF4 channel. Pane 1 shows the three layers A, B and C. A represents the spacer (200 - 500 µm), B represents the ultrafiltration membrane (permeable wall) and C represents the frit. Pane 2 shows the insertion order for channel assembly and pane 3 shows the assembled channel from the side. The XCT slice direction is indicated in the schematic. Rotating the slices 90 degrees shows the schematic view of the XCT slices. The elution channel volume is defined by the trapezoidal-shaped hole in the spacer, by the channel top and by the ultrafiltration membrane at the bottom (14).

The name Asymmetrical flow field flow fractionation describes the technique very well for the initiated reader. Breaking down the name, word by word, may clarify the meaning and explain the technique step by step and in a bigger picture.

Asymmetrical refers to the property of having only one permeable wall (5). Historically channels were constructed with an upper permeable wall as well as a lower one (20, 21). The asymmetry can also be attributed to the shape of the channel, and the flows in and through the channel. A trapezoidal shape of the channel was introduced to reduce the effect of loss of volumetric carrier flow rate downstream the channel, due to crossflow passing through the membrane (6). Originally the channel shapes were rectangular. With a trapezoidal shape the carrier flow velocity is maintained downstream and throughout the analysis. In other words, the tapered shape reduces the risk of stagnant analytes, causing longitudinal band broadening and mixing of sample zones, as they move towards the outlet.

The first mention of flow in the name of AF4 refers to the separation field, the **flow field**. The flow field in AF4 is constituted by the crossflow. The family which AF4 belongs to has other members with different types of separation fields, e.g. electrical, sedimental, and thermal. In all cases the field is applied perpendicular to the direction of analyte motion or elution direction and across the channel height. Common for all the members is the use of a flow, driving the analytes forward in the fractionation device, and that's the reason for the second mention of **flow** in AF4 and why it is called flow fractionation.

Fractionation then, and why not separation? Well, this can be debated, AF4 is clearly also a separation technique. E.g. in the case of a two-component sample system with a large enough size difference between populations, these can be baseline separated by AF4. Isolated individual components from a complex mixture can be achieved by AF4. Historically, and still, common use of AF4 involves fractionation of a continuum of sizes, where the resolution does not allow baseline separation, but rather fractionation. Fractionation is a separation process where a mixture is divided into fractions, based on e.g. physical properties like size or mass, and where each fraction is enriched in certain components. Fractions of the eluting sample, with for example a narrow size range within, can then be collected by a fraction collector.

The purpose of the crossflow has been mentioned above and of course in this chapter the laminar channel flow also needs introduction. It is the combination of crossflow and laminar elution flow which concludes fractionation of analytes. Referring to figure 1, the laminar flow is represented by the parabolic flow profile. In figure 1, l is the average height position of a certain size above the ultrafiltration membrane, F_{in} is the volumetric channel flow into the channel, F_{out} is the volumetric channel flow out from the channel, F_{cross} is the volumetric channel crossflow, and w is the channel height (Q is also commonly used for volumetric flows). These are all parameters affecting separation and retention times. The sample is injected through a dedicated sample injection port, a few centimetres downstream from the channel inlet. The first step in a separation method is to focus and relax the sample. Focusing is a flow-induced collection of the sample plug to a spot or a band, a few centimetres downstream from the sample injection port. During the focusing there is no flow leaving the channel through the channel outlet, but only through the membrane in the bottom. The flow is directed into the channel through the inlet and the outlet simultaneously, creating a focusing spot as the two flows with opposite directions meet, and at the same time creating a flow induced transport and forcing the sample towards the membrane. When the sample is in the focused state, a relaxation of the sample occurs. While being forced towards the membrane by the crossflow, diffusional transport is working in the opposite direction. Eventually the sample will reach a relaxed state where each size portion of the assembly will reach a diffusion coefficient dependent average height, l, above the channel bottom (the membrane), sometimes also called the accumulation wall. When the sample has relaxed, the direction of the outlet flow is switched, and elution starts. The flow, which is now going through the channel is laminar and has its highest flow velocity in the centre of the channel. At the top and bottom of the channel the flow is almost stagnant. This means that the laminar flow will have a parabolic flow profile, see figure 1. The sample fraction having the highest average relaxed height above the accumulation wall, l, will experience the highest flow velocity in the parabolic flow profile and thereby elute earliest. The higher the diffusion coefficient the higher the position and elution order will therefore be by smallest first. The outlet flow is sometimes referred to as channel flow or detector flow. Detector flow is perhaps the

better description, since detectors normally are connected in series to the channel outlet. At the Department of Process and Life Science Engineering the AF4 is typically connected to MALS (for determination of size, radius of gyration - r_g, or root-mean-square radius - r_{rms}, and molecular weight, M_w), UV and RI (for concentration detection). A typical AF4 setup is illustrated in figure 3.

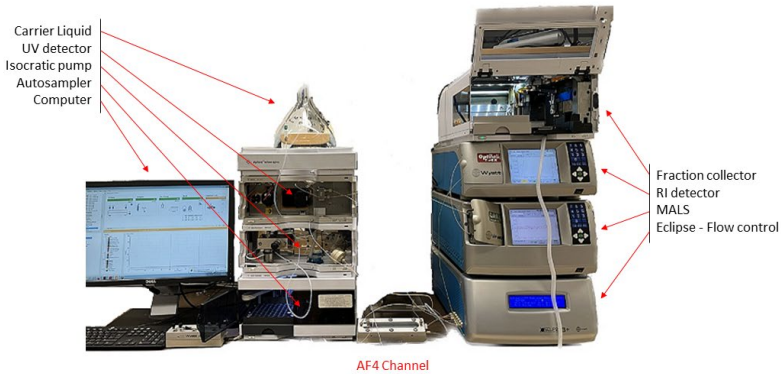

Fig. 3. A typical AF4 setup with components from left to right, computer/software, LC-rack (with isocratic pump, autosampler, UV-detector and carrier liquid on top), AF4 channel, Eclipse 3+ for channel flow control, RI- and MALS-detectors, and fraction collector on top.

When working out a fractionation method in AF4 there are several things to consider. The crossflow needs optimization, a too low crossflow will compromise separation, while a too high will extend retention, causing broadening of the sample zones and potentially overlapping (see also retention level below). Typical values range from 0-10 ml/min. The usable range of crossflows is always limited by the hardware configuration of the instrument used. It is common procedure to utilize dynamic crossflows during separations, especially for samples with wide size distributions. Both linearly and exponentially decaying crossflows are deployed for various separations.

A detector flow of 0.5 – 1.5 ml/min is common today. The detector flow will affect retention times and e.g. for large aggregates or high molecular weight polymer separations an increase may be necessary. The best resolution is always achieved using the highest possible detector flow and crossflow, but the maximum detector flow is limited by the counter pressure exerted by the on-line detectors. As for all separation techniques using gas or liquid as carrier, broadening of the sample plug is time dependent. The longer the retention, the wider the broadening of the sample plug and the lower the resolution.

The retention parameter used in AF4 is called the retention level, R_L. The retention level is defined as the ratio between retention time, t_r and void time, t^0,

$$R_L = \frac{t_r}{t^0}, \quad \textbf{(1)}$$

and by empirical evaluation it has been concluded that separations agree well with elution theory for AF4 when R_L falls between approximately 5 and 30 (17). This should always be considered for method optimization. Every rule of thumb has exceptions though and is true also for this case. As an example it has been shown that the albumin dimer could be eluted according to theory at R_L ~70 (17).

The channel height, *w*, needs consideration as well. Typical heights range from 200-500 µm. With a higher channel, higher resolution can be achieved, due to a lower detector flow velocity gradient, *dv/dh* (where *v* is the flow velocity and *h* is the height above the accumulation wall), but consequently retention time and dilution of the sample will increase.

The carrier liquid options are often mentioned as an advantage of AF4 compared to other techniques. The reason is that the carrier liquid can, in most cases, be chosen to fit the required sample demands or if you like, to fit and achieve the demanded sample state. Most separations are performed in buffer carriers with varying pH and ionic strengths.

The channel area is also a retention time-affecting factor. Channels with varying lengths and widths exist. With a lower width channel, higher maximum flow velocities are achieved with identical hardware configuration. The pump and flow device configuration may be a limiting factor due to maximum achievable volumetric flow. To compensate for this a smaller channel area is useful to increase crossflow velocities. The breadth of the channel is related to how much sample can be loaded, and a wider channel can allow for somewhat higher sample mass loading. With a wide channel it is also more likely to avoid edge effects during relaxation and elution.

When optimizing a method, it is also important to consider the sample load. Injecting a too high mass of sample can compromise the relaxation and thereby the separation, i.e. overloading. At overloading there is not room enough for sample components to take their relaxed average height equilibrium position according to diffusion coefficient. This can be identified as fronting peaks and poor size separation looking at the detector signals. At the same time, it is of interest to inject as much sample as possible to have adequate amount of sample to detect. For on-line coupling to SAXS, this cannot be stressed enough.

Last, but not least in this chapter, it should be said that AF4 has advantages in the separation procedure due to the void of stationary phase. This fact means that samples will be subjected to less stress, i.e. shear stress, when not being squeezed

through a closely packed column for example. The void of stationary phase also means lower surface area for the sample to interact with, whether leading to accelerated aggregation, degradation, or adsorption.

Sometimes AF4 is mentioned as a chromatography-like technique. AF4 is not chromatography, due to the void of a stationary phase in the separation device. The resemblance to size exclusion chromatography (SEC) or liquid chromatography (LC) comes from the fact that fractionations/separations are performed in liquid carriers. Analytes are dispersed/dissolved in a liquid prior to injection and are carried by an elution flow towards the channel outlet.

Size fractionation techniques

Size fractionation techniques for applications in the nano, micro, and macro ranges exist. Probably the oldest and still quite frequently used is the sieving approach, where sieves in consecutive mesh sizes can be used to sort everything from rocks and gravel to micronized material e.g. in the pharmaceutical research and production steps. The result from sieving is either a size-sorted assembly or, in the utilization of a stack of sieves, an estimation of size distribution. The result and resolution of sieving is dependent on the mesh-size difference between sieves. Consideration is needed to the initial and the final mesh-size, since everything which is larger than the largest mesh or smaller than the smallest mesh will not be sorted. This unsorted material is referred to as the excluded volume.

Other size fractionation techniques commonly used are e.g. cyclones, crystallization, and sedimentation. The importance of size fractionation arises in many fields and applications. To mention something of relevance for this thesis, in the pharmaceutical field, size distribution analysis is performed to assess properties like porosity and compressibility, flowability, dissolution rate, and to verify the oligomeric state of molecules.

Determination of the distribution of sizes or molecular weights in an assembly in the nano-micro range has importance for characterization and quality control. Average values, or biased results, which is the outcome of some size characterization methods, may not be sufficient. Dynamic light scattering (DLS) in batch mode for example is a fast and common method for determination of hydrodynamic diameter but is biased towards larger sizes (16, 22). The biasing compromises the true state of size distribution within a sample. In this thesis the importance of size fractionation is exemplified in paper II, by the AF4-SAXS coupling, where antibody conformational differences are found between two size fractionated populations in the assembly.

Samples in the nano to micro range are impossible to size fractionate using ordinary mechanical sieves. For the required resolution in these size ranges other techniques and interactions are necessary to apply. For molecular resolution in the size fractionation, here will be mentioned three main techniques for physical size-separation and characterization, or determination of particle size distribution (PSD) or molecular weight distributions. AF4-MALS is one of them, Size Exclusion Chromatography coupled to MALS (SEC-MALS) is another and Analytical

Ultracentrifugation (AUC) a third. All of which have their limitations and pros and cons, see table 1.

SEC and AF4 are both dependent on a stable carrier flow from isocratic pumps and the systems are similar in their configurations. Between the pump and the separation device normally sits an autosampler for automatic sample injection and the separation device is then coupled in series to one or a few detectors, choices which are made depending on application and requested results. The main difference is the construction of the separation device. The somewhat more complex configuration and control of the AF4 channel requires a separate device for controlling the flows inside the channel.

The SEC separation device is a column filled with a close packed material, porous gel beads, which allows for particle passage between them. This results in higher pressure during separation compared to AF4. The gel beads are porous to a certain depth which allows for column specific sizes to enter the pores and to travel in-and-out of pores. The flow velocity in these pores differs from that in the shortest path through the column. This is important since the separation mechanism and selectivity is based on the path length travelled through the column, which in principle is decided by the residence time in the pores. Large species will not be able to enter the pores of the close packed material and will have lower retention since they will travel in a straighter and shorter path through the column. This part of the sample becomes, equivalent to the sieving process, part of the excluded volume. Therefore, it is of crucial importance to choose the column based on the size or molecular weight of the sample. The column specification will contain information about the useful range of molecular weights. The lower size limit is set by the pore size and sample components that are small enough to enter all pores will end up in the so-called permeation limit (compare to smallest mesh size in sieving). Sizes lower than the permeation limit will elute together in a band. SEC is sometimes also called molecular sieve chromatography.

One limitation with SEC is the ability to determine the amount of aggregation in e.g. a protein biopharmaceutical. Aggregates can be too large to filter through the closely packed column and consequently block the column or end up in the excluded volume. Another limitation is the need for concentration reduction of the injected sample. Concentration reduction may falsely alter the aggregation concentration of reversible self-assembly of proteins. This problem is also true when AF4 is used for determination of aggregational state. The cause being dilution of the sample, which will happen in the AF4 channel as well as in the SEC column. However, in AF4 it is possible to inject higher initial masses, which are then focused before elution. In SEC the sample is injected in a thin sample plug and separated right away.

Analytical ultracentrifugation subjects the formulated sample to a centrifugal field where sedimentation rate is observed using optical detection like UV, refractometry and fluorescence. The sample is contained in a vial throughout the course of the

analysis and a sample can be kept under optimized formulation during the complete analysis. The sample concentration can be kept at the desired level and altered between runs as well. Molecules can be quantitively monitored and size characterized during the centrifugation process. Fraction collection is not possible though, like in AF4 and SEC, but the molecular weight range can be determined. The molecular weight range measurable by AUC ranges from a few hundred kDa to 10^9 kDa. Sedimentation rates can be altered by adjusting the rotational speed and the centrifugal force subjecting the sample. The most obvious cons with AUC, apart from the fact that no fraction collection is possible, are the long measuring times and the demanding analytical calculations, which require plenty of time as well. For characterization of biopharmaceuticals, for which AUC is mostly used nowadays, AUC is a useful orthogonal technique used for verification of SEC and AF4 methodology and results. Especially for SEC methodology, with unpredictable results for samples prone to aggregation, which originates from the large surface area of the SEC column and the shear stress induction during elution. Consistent results from orthogonal techniques are something to always aim for when dealing with size distribution characterization.

Table 1. Comparison of properties for three common fractionation/separation/particle size distribution techniques, AF4, SEC and AUC.

	SEC	AF4	AUC
Analysis range	Small-intermediate size <50 nm	Small-large size (limitations in smaller sizes or < 10 kDa)	Small-large
Method development	Easy	Easy-challenging	Intermediate-challenging
Sample prep time	Short	Short	Relatively long
Experiment time	Intermediate	Intermediate	Long-very long
Data analysis complexity	Easy-intermediate	Easy-intermediate	Intermediate-challenging
Data analysis time	Short	Short	Long
Internal surface area	Very large	Small	Smallest
Shear forces / pressure	High / ~100 bars	Low / ~10 bars	Low / ~1 bar
Dilution in analysis	Intermediate	Intermediate/ influenceable	Very low
Carrier liquid compatibility	Yes, but modifications common to avoid interaction (salt, co-solvent, glycine, histidine)	Yes, mostly hardware dependent, modifications may be necessary	Yes
Fraction collection	Yes	Yes	No
Cost of equipment	Low	Intermediate	High

AF4 Calibration (R_H determination)

The calibration of the AF4 channel is performed for the purpose of determining the channel height and to use this value for determination of hydrodynamic radii, R_H. With knowledge of the channel height, the hydrodynamic radius can be calculated for every retention time and thereby over a complete fractogram. The hydrodynamic radius or the Stokes - Einstein radius (23) is related to the translational diffusion coefficient, D, by the following inverse relationship,

$$R_H = \frac{k_B T}{6\pi\eta D}, \qquad \textbf{(2)}$$

where k_B is Boltzmann's constant, T is the absolute temperature, and η is the dynamic viscosity of the medium where the diffusion happens. The hydrodynamic radius is the radius of a perfect sphere in the derivation of eq. 2 and for samples with arbitrary shapes and/or irregular surface, R_H should be interpreted as the equivalent size of a sphere having the same diffusion coefficient as the sample under investigation. In other words, R_H is not a comprehensive description of samples deviating from spherical, but rather one of many ways of describing size of such.

To determine the channel height, one way is using a sample of known hydrodynamic size which is eluted under known circumstances (24, 25). The retention equation for AF4 relates retention time, t_r, to hydrodynamic radius, R_H and channel height, w,

$$t_r(D, w) = R_L(\alpha, \lambda)\frac{\lambda w^2}{D}\ln\left(1 + \frac{V_C}{V_{out}}\left[\frac{A(z')}{A_{tot}}\right]\right), \qquad \textbf{(3)}$$

where $\alpha = R_H / w$, $\lambda = l / w$, l is the average sample height in the channel, V_C is the crossflow, V_{out} is the detector flow, $A(z')$ is the accumulation wall area up to the focusing point, and A_{tot} is the total accumulation wall area.

To solve the equation by implicit numerical methods, and to determine w, a calibration experiment must be performed. In the calibration run the retention time is measured at a constant V_c / V_{out} ratio, while the hydrodynamic size of the analyte must be known.

A calibration experiment is typically performed using a small sized protein or particle, like bovine serum albumin, ferritin, or standard particles, with known hydrodynamic sizes. As mentioned in the introduction this is a somewhat criticized

method since it results in a one-point calibration. To make the calibration more robust, paper I suggests using an oil-in-water nano-emulsion instead. A nano-emulsion consists of nanosized oil droplets which can be size distribution determined, following fractionation, using light scattering theory, by MALS. The geometrical radii measured can be estimated to equal the hydrodynamic size, since the oil droplets are spherical and covered only by a surfactant monolayer. In one measurement the hydrodynamic radii and corresponding retention times can be determined, and eq. 3 can be solved using non-linear regression. The result is a channel height determination based on multiple sizes, or retention levels. In the paper, the result from the novel nano-emulsion calibration method is orthogonally compared with X-ray computed tomography (XCT) imaging of the channel as well as to standard particle calibrations with consistent results for *w*. The nano-emulsion method is evaluated for a set of constant crossflows to really cement the robustness of the method. Furthermore, the calibration method is tested for low and high pH, for which the size of proteins or standard particles would be inconsistent.

Paper I is an example of method development where orthogonal techniques were used to answer the question stated in the AF4 critical overview by Wahlund (17), where it is suggested to use a range of sizes to check the consistency and robustness of the calibration. What better way to do it than by using a single sample with a wide size distribution and to fit the resulting elution to elution theory. The con is of course the hassle of using numerical methods for equation solving. To work around the usage of numerical methods, which may not be easily accessible for every user, it is possible to create a calibration curve using several known hydrodynamic sizes. This procedure is time consuming though and costly to keep a stash of standard particles or proteins. The nano-emulsion method is relatively fast and more cost effective since the nano-emulsion can be made from standard chemicals, by using standard chemical laboratory equipment, and has a long shelf-life.

To solve equation 3, it is necessary to determine $A(z')$. This is performed by injection of a dye, which under focusing visually shows the focusing point. The focusing position is for existing calibration methods measured manually using e.g. a calliper, after which the area upstream the focusing point, $A(z')$, can be calculated. Manual measurement of the focusing point has the potential of introducing an error (3 mm off, results in an error of approximately 1%, in *w*) in the solution to the retention equation, eq. 3, which is why arguments for better methods of *w*-determination have emerged. Hopes stand to technical developments of optical methods for *w*-determination, instead of using standard particles, proteins or nano-emulsions for calibration experiments (26). The main influencing factor for introduction of errors in the determination of *w* is however the void time, t^0 (26), which is why it is recommended to calculate the void time for an unretained entity using eq. 4, instead of trying to identify the time from the fractogram. The origin of the often so-called void peak is not clearly understood (17).

$$t^0 = \frac{V^0}{F_{cross}} ln\left(1 + \frac{F_{cross}}{F_{out}}\left[1 - \frac{w\left(b_0 z' - \left[\frac{(b_0 - b_L)}{2L}\right] z'^2 - y\right)}{V^0}\right]\right) \quad \textbf{(4)}$$

(b_0 and b_L breadths of the trapezoid defining the channel geometry, z' the focusing point position, L the channel length, y is the area lost from the trapezoid by the tapered inlet and outlet, V^0 is the channel volume)

Small Angle X-ray Scattering

X-ray scattering is a static scattering technique which can be used to measure size, molecular weight, shape, and structural information of material/matter. In dilute systems, small angle X-ray scattering (SAXS) can be used to determine the size and shape of dispersed particles or molecules and the arrangement of material within them (27, 28). In a concentrated or solid system X-ray scattering can be used to measure spatial arrangements between scattering centres.

The fundamental reason for scattering occurring is the interaction of radiation with electrons. Local fluctuations in dielectric constant throughout the medium where the light incidents, are prerequisites for angular dependence of scattered light. The intensity of scattered X-rays scales with e.g. electron density and wavelength of the incident light according to Rayleigh (29), as λ^{-4}.

In SAXS, as the name implies, X-rays are scattered of scattering centres in the sample under investigation and the corresponding interference pattern created by the scattered X-rays can be used to identify characteristic properties of the sample. X-rays have a wavelength in the same order as the size of atoms (~ Å); they can interact with the electron clouds of individual atoms and molecules. It is generally so, that accessible sizes scale with the wavelength of the incident light. MALS, which is commonly coupled on-line to AF4 for size determination, has a lower limitation in accessible diameter size range at approximately 20 nm. This is due to the usage of visible light. For small sized proteins or particles, or for other features at the same length scale, scattering shows no angular dependence in the visible light scattering regime. Thus, to access characteristic light scattering data from AF4-eluted sample of sizes below 20 nm, the AF4 needs to be coupled elsewhere, e.g. to SAXS which has a lower spatial limitation at approximately 1 nm. SAXS, unlike visible light scattering, also offers more comprehensive information about shape and structure.

The angular dependence of scattered light is what makes it possible to estimate the size, shape, and structure of a particle or molecule. When scatterers show no angular dependence in the light scattering, they are isotropic scatterers and scatters light with identical intensity in all directions. A sample can also be isotropic in the sense that the scattering pattern shows concentric circles (figure 4). This is true for example for a protein solution which consists of randomly oriented scatterers.

The angular dependence traces down mathematically to the scattering vector q, which is the difference in propagation vectors of incident and scattered light (see figure 4). In standard SAXS experiments elastic scattering is considered and

$$q \equiv |\boldsymbol{q}| = \frac{4\pi}{\lambda} sin\frac{\theta}{2}, \quad \textbf{(4)}$$

where λ is the wavelength and Θ the scattering angle. In a SAXS experiment the scattered light intensity, $I(q)$, in different angles, q, is acquired using a two-dimensional detector and after radial averaging, results are presented in 1-dimensional $I(q)$ vs q plots. The radially averaged 1D intensity has the general expression,

$$I(q) = \Phi \cdot V \cdot \triangle \rho^2 \cdot P(q) \cdot S(q) + B \quad \textbf{(5)}$$

where Φ is the volume fraction of particles or molecules, V is the scattering volume, $\triangle \rho^2$ is the difference in scattering length density between solvent and solute, $P(q)$ is the form factor, $S(q)$ is the structure factor, and B is the background arising from incoherent scattering. The form factor $P(q)$ describes intramolecular interference and is consequently describing size and shape. The structure factor $S(q)$ describes the interference from interparticle interactions. In a bulk measurement using SAXS the concentration of solute is normally reduced to a degree where the structure factor can be ignored. $S(q) \rightarrow 1$ for dilute systems and for sample eluting from the AF4 channel the concentration is normally below this limit (although this is sample dependent).

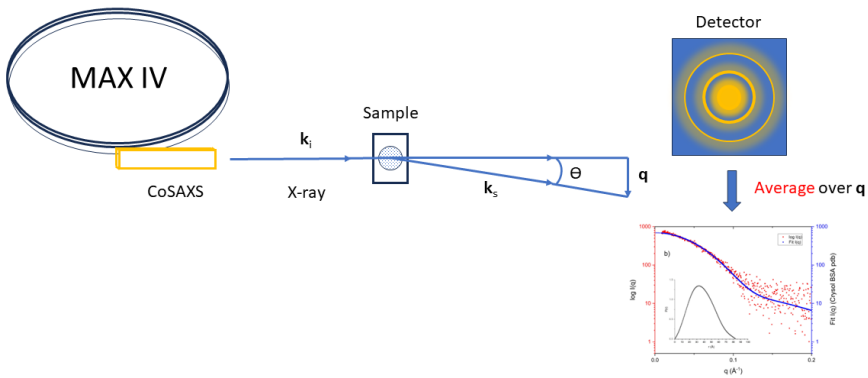

Fig. 4. Schematic explanation to scattering vector q and the transfer from the acquired 2D intensity to average 1D intensities as function of q.

The *I(q)* vs q graph is e.g. used for model fitting to existing models. Knowing the sample system well is key for unordered systems (e.g. proteins and biomolecules). Scattering curves can be quite featureless, but by a carefully considered model choice and reduction of the number of fitting parameters, the fitting can be done with higher confidence. The regime where *I(q)* is independent of q (extrapolated to *I(0)*) is proportional to molecular weight and concentration of analyte. If the concentration is known the molecular weight can be determined. Besides molecular weight, several parameters can be obtained from the SAXS curves (30-32), such as excluded particle volume or Radius of gyration (R_g) (27).

Other information about the system can be derived, using the Kratky plot and the Pair distance distribution function.

Kratky Plot

The Kratky plot can be used for qualitative assessment of the flexibility or degree of disordered arrangement of proteins or other flexible molecules. The idea of plotting

$$q^2 I(q) \; vs \; q,$$

was introduced by Otto Kratky (28) for such assessments. Globular proteins show scattering intensity decay rates of q^{-4} and flexible chains show decay rates of q^{-2} or less in the so called Porod region. By visual inspection of the Kratky plot a compact molecule should show $q^2I(q)$ values approaching zero for higher q, while a flexible conformation should plateau at intermediate values of q and possibly approach infinity for higher q. An intrinsically disordered protein will show $q^2I(q)$ values approaching infinity for high q.

An alternative normalized version of Kratky plot is the

$$\left(qR_g\right)^2 I(q)/I(0) \text{ vs } qR_g.$$

These plots are dimensionless and e.g. a folded globular protein will show a maximum at 1.1 for $qR_g = \sqrt{3}$. See figure 5.

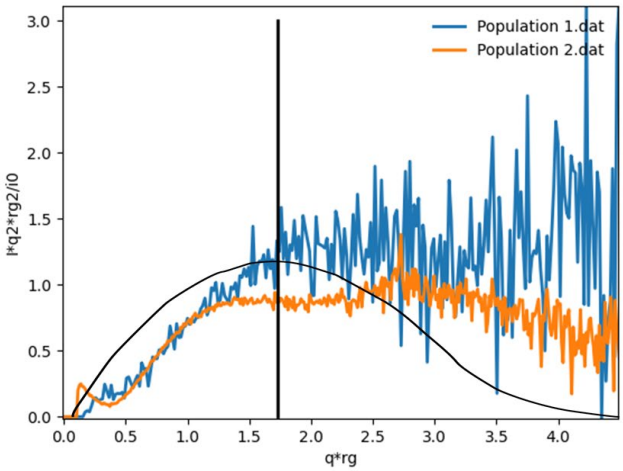

Fig. 5. q^2-Normalized Kratky plots for two different proteins. The blue curve shows a very flexible protein, and the orange shows a protein that has both globular and flexible parts, getting closer to 0 at higher *q*. In black, the typical globular protein shape, with a defined peak and approaching 0 for high *q*. The black vertical line indicates $q*R_g = \sqrt{3}$, where globular proteins have their maximum.

Pair distance distribution function, *P(r)*

The pair distance distribution function, *P(r)*, is used in SAXS analysis to extract real space data from the scattering profile, which is measured in reciprocal distance space, or *q*-space (28). The indirect Fourier transform of the scattering data gives *P(r)*, representing the frequency of distances between any two scattering centres within the sample. By iteration and boundary conditions set, the maximum distance between electrons in pairs within the sample body, D_{max}, can be found. D_{max} represents e.g. the diameter of a spherical sample or the length of a rod-shaped object. From the shape of the *P(r)* function, conclusions about the shape of samples can be drawn. See figure 6.

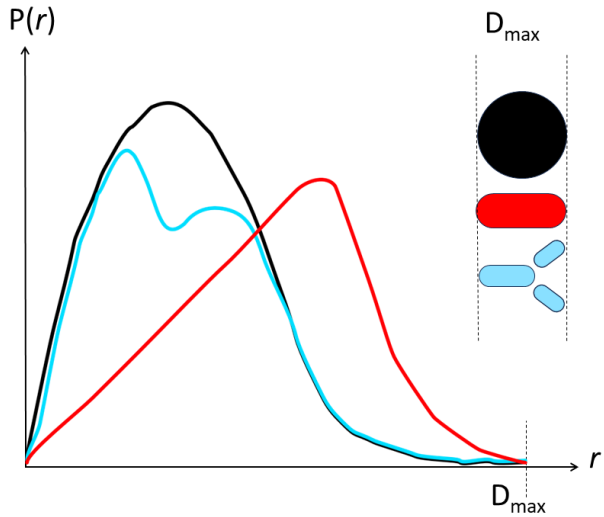

Fig. 6. Pair distance distribution functions for three common sample shapes. In black, spherical, typical for globular proteins. In red, a typical shape for a rod-like sample, and in light blue the typical *P(r)* shape of an antibody.

AF4-SAXS in on-line coupling

In paper II, SAXS in on-line coupling to AF4 was demonstrated as a useful tool for the characterization of biological molecules. When SAXS is used in the application field of biomolecules, the technique is abbreviated BioSAXS. Biomolecules are generally weak scatterers of X-rays due to low electron density. In combination with AF4 it becomes important to maximize sample load and photon flux, since AF4 also dilutes the sample. The on-line coupling of AF4 to SAXS was performed at MAX IV Laboratory and the beamline CoSAXS. The benefit of using a synchrotron source of x-rays depends on the flux, the number of photons per second. In comparison to a benchtop SAXS instrument, the photon flux at a synchrotron is approximately 10^5-10^7 higher. This means that acquisition rates are shorter, which is necessary for sufficient collection of intensities from an eluting sample, in constant motion. The scattering volume is constantly moving through the positioned x-ray beam.

The most common way of performing BioSAXS is in batch mode. This requires a highly monodispersed sample, and minute preparations to present solutions of only background (e.g. buffer) and buffer + sample. The contamination of sample solution may deteriorate the results, since the scattering from unwanted content will result in a sum-weighted scattering pattern from every scatterer in the sample. The scattering from a collection of sizes and shapes is difficult to interpret correctly. For the same reason it is not possible to measure a formulated sample in batch mode and to expect separate results and characteristics of each component.

The profound reason for coupling a fractionation instrument on-line for detection is to be able to take a ready formulated sample containing many components and conformations, and to analyse the formulation in-situ and as direct as possible. The fractionation instrument separates continuously and presents to the detector a minimum amount of diversity in sizes at every instant. The coupling of AF4 to SAXS has the potential of providing previously hard to reach characteristics of formulated samples. The main applicability lies within samples with wide size distributions and with fractions in the large size range. AF4 is also the preferred choice for samples which are sensitive to shear stress and surface interactions. The versatility in the choice of carrier liquid is another benefit of AF4, since it allows to adopt the carrier liquid to the sample rather than to the compatibility with instrumental parts or to avoid interactions. SEC has previously been coupled to SAXS and SEC-SAXS is available at synchrotron sources globally. For successful separations using SEC it is however sometimes necessary to alter the carrier liquid by additives to prevent interaction with the porous gel beads in the column. SEC also has a limitation of separation in the larger size range, above approximately 50 nm.

Results from Paper I and II in summary

In this chapter the results from paper I and II will be presented in a summarized overview. Readers are directed to read the full versions of the articles to seek answers to specific details.

Paper I

In paper I, a new method for calibration of the AF4 channel height is evaluated. The use of a nano-emulsion, with a wide particle size distribution, instead of the one-particle calibration procedure is aimed to make the calibration more robust. With a nano-emulsion, a range of sizes can be used for the calibration in a single experiment. Figure 7 shows the fractograms for a nano-emulsion eluted under different constant crossflows, ranging from 0.2 to 0.8 ml/min. Retention time is proportional to the crossflow according to eq. 3. The circles in figure 7 represent the geometric radii, determined by MALS, of the oil droplets in the emulsion. The geometric radii are here approximated to equal the hydrodynamic radii, since the thin layer of surfactant on the droplets can be neglected. The dashed lines are, through elution theory, the fitted curves to the elution of sizes, by iteration of the channel height, *w,* in a non-linear regression.

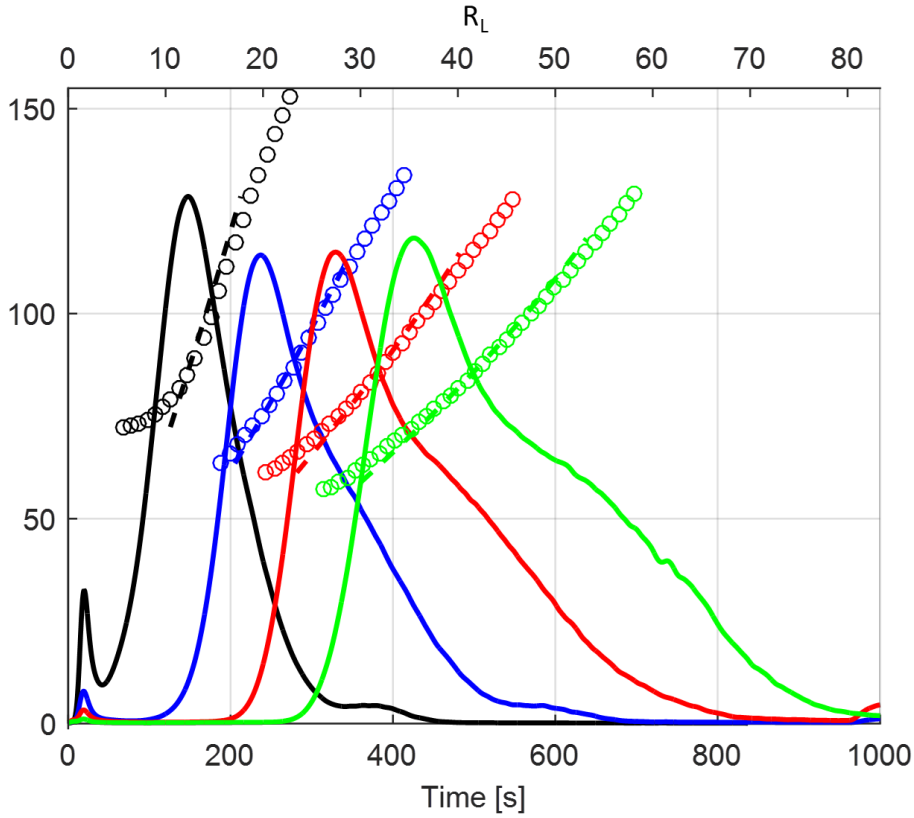

Fig. 7. Experimentally determined nano-emulsion elutions at constant crossflows 0.2–0.8 ml/min. Circles represent the experimental elution profile, dashes represent the elution model (eq. 3)

Table 2 shows the calibration results using the nano-emulsion method in four different AF4 channels, and at pH 5, 8.5, and 10 respectively. The results are consistent in the crossflow range used, with relative standard deviations between 0.7 and 2.5 %.

Table 2. Channel height calculation results from four different channel assemblies, run at three different pH values. In pH 8.5, A and B denote two different channel assemblies.

		pH 5	pH 8.5		pH 10
Crossflow (ml/min)		**Channel height (µm)**	**Channel height (µm)** A	B	**Channel height (µm)**
0.2		210 (R_L=9)	163 (R_L=8)	176 (R_L=7)	183 (R_L=7)
0.4		208 (R_L=18)	161 (R_L=15)	172 (R_L=13)	180 (R_L=13)
0.6		216 (R_L=28)	164 (R_L=23)	172 (R_L=18)	183 (R_L=19)
0.8		216 (R_L=42)	163 (R_L=30)	175 (R_L=24)	192 (R_L=27)
	Mean	213	163	174	185
	Std	3.5	1.2	1.8	4.6
	CV (%)	1.6	0.7	1.0	2.5

The nano-emulsion calibration method was validated utilizing the determined channel height to calculate hydrodynamic radii of standard polystyrene particles. The same particles were also size determined using MALS, and the measured geometric radii were compared to hydrodynamic radii from elution theory calculations. Results are shown in table 3. The % error was below 10% as long as $R_L < 30$. It has been shown experimentally that elution theory works well in most cases when the retention level is kept below 30 (40 is sometimes mentioned). This is not universal, but extra care should be taken when long elution times are used. The longer residence time in the channel, the higher the risk that approximations in elution theory and other effects like interactions get to play a bigger role in the movie than the researcher wishes.

Table 3. Validation experiments using standard particles (PS60, PS100 and PS200) in three different channel assemblies (at two different carrier liquid pH values). r_{geo} is the radius determined by the MALS detector, r_h is the hydrodynamic radius determined by the retention theory and the mean channel height (determined in the nano-emulsion experiments with different crossflows.) A and B denote two different channel assemblies with the same carrier liquid.

pH	*w* [µm]	Q_C[ml/min]	Q_{out} [ml/min]	r_{geo} from MALS [nm]	r_h determined from retention theory [nm]	% Error	R_L
8.5(B)	174	2.0	1.0	33	32.7	-1.4	11
10	185	2.0	1.0	33	37.5	13	44
10	185	2.0	1.5	33	40.7	23	40
8.5(A)	163	0.4	2.0	51	52.6	3.1	8
8.5(A)	163	0.6	2.0	51	52.6	3.1	12
8.5(A)	163	0.8	2.0	51	53.4	4.7	16
8.5(A)	163	0.4	2.0	101	106	5.0	15
8.5(A)	163	0.6	2.0	101	110	8.9	22
8.5(A)	163	0.8	2.0	101	118	17	30

For orthogonal validation, one of the channels was also imaged using X-ray computed tomography (XCT). See figure 8. Figure 2 additionally explains the orientation of the XCT image in figure 8. Results from image analysis of the tomography images are shown in table 4. The result from the direct imaging of the channel height fits well to the channel height determined by the nano-emulsion method. The channel used for XCT imaging was filled with carrier liquid at pH 5 and equipped with a 250 µm thick spacer.

Table 4. Results from image analysis determination of channel height from XCT.

	1	2	3	4	5	6	7	8	9	10	11	Mean	Std
Height (µm)	213	207	207	201	213	213	207	201	213	213	207	209	4.5

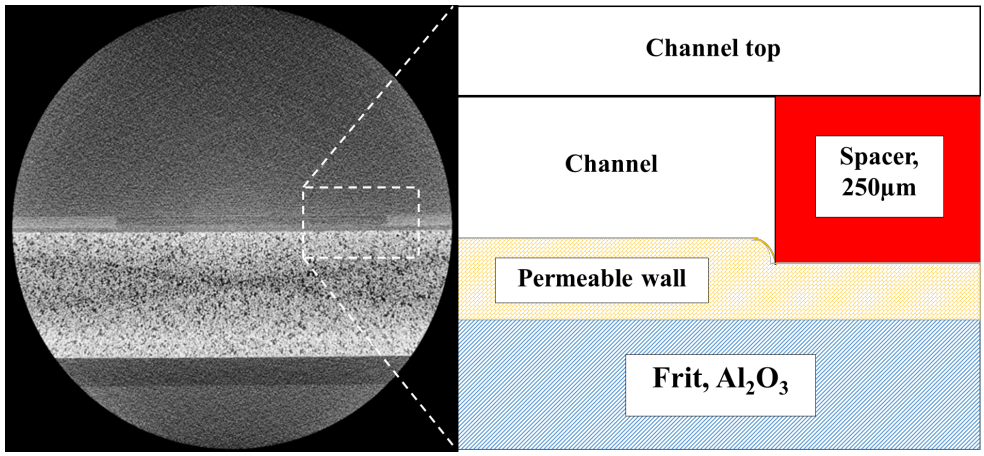

Fig. 8. Left: XCT image of the channel assembly. Right: Magnified schematic of the visible parts.

Paper II

In paper II the on-line coupling between AF4 and SAXS is evaluated for applications on biologics and specifically on proteins. Biomolecules are generally weak scatterers of X-rays and for this evaluation AF4 has been coupled to the CoSAXS beam line at MAX IV Laboratory, to make use of the high flux of X-rays available only at synchrotron sources, and to be able to collect adequate SAXS data at every instant of a weakly scattering sample eluting at a constant flow rate from the AF4 channel. The model systems used for the realization of this new method was BSA and the antibody Trastuzumab. Figure 9 shows the normalized average intensity of scattered X-rays and the normalized UV intensity as a function of elution time for BSA. From figure 9 it is concluded that the method works, the band broadening in the SAXS capillary is negligible and the S/N is good for extracting data, exemplified in figure 10.

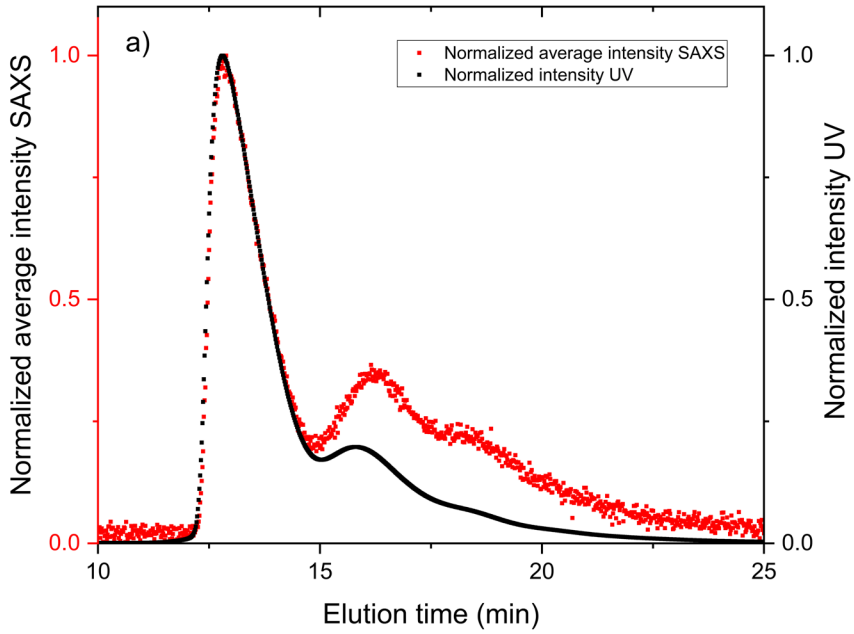

Fig. 9. Fractogram of BSA, 300 µg injected, with peak-maximum normalized average intensities of SAXS (red) and peak-maximum normalized intensity UV absorption at 280 nm (black) vs time.

An attractive feature from separation prior to SAXS, i.e. AF4-SAXS, is that the background can be extracted from parts of the elution profile where no sample is eluting, but only carrier liquid. Figure 10 shows the *P(r)* for the BSA monomer and the corresponding fit to the crystal structure scattering data of BSA.

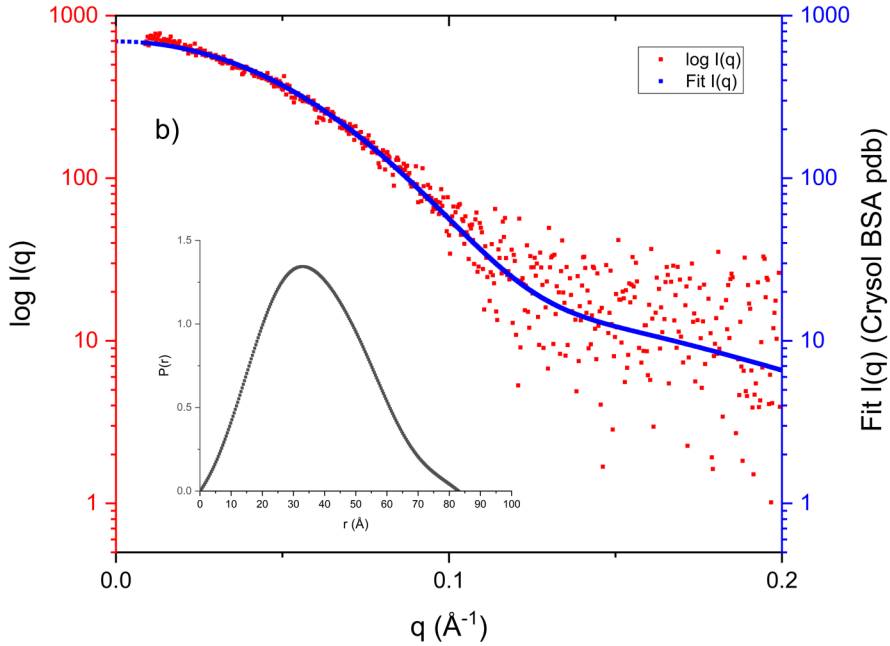

Fig. 10. SAXS data (red) from the monomer peak of BSA and the corresponding fit to the crystal structure of monomeric BSA (blue) in a log *I(q)* vs *q* plot, *P(r)* vs *r* inset.

In a typical AF4 fractionation of a protein, which forms dimers and higher order oligomers in solution, a sample mass of about 30 µg is injected. Figure 11 shows injections of 60, 150 and 300 µg injections of BSA. An increasing loss in resolution and tendency towards overloading can be observed for the two higher masses, but separation is still achieved. To evaluate the dimer of BSA, it was necessary to inject a higher than typical sample mass for adequate SAXS signal detection.

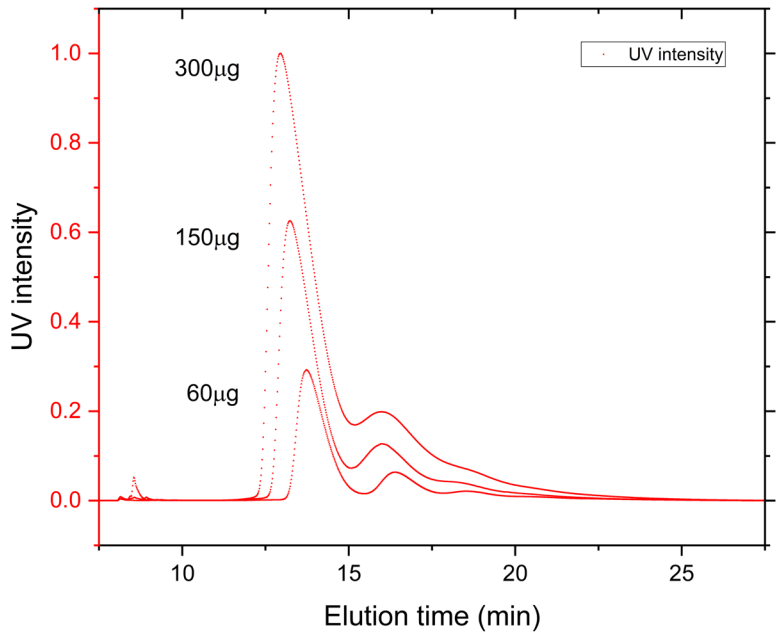

Fig. 11. UV fractograms of BSA injected at 60, 150, and 300 µg. The injected masses of 150 and 300 µg show decrease in resolution and slightly shorter elution times, approximately 45 s, due overloading.

Figure 12 shows the fractogram of Trastuzumab, 300 µg injected. For this sample, two populations were observed, which was unexpected. In paper II, the origin of the two populations was derived. First a deglycosylation of the antibody was performed to rule out the origin to be a difference in glycosylation patterns. Figure 13 shows that a general and identical decrease of molecular weights over the two populations occurred after deglycosylation.

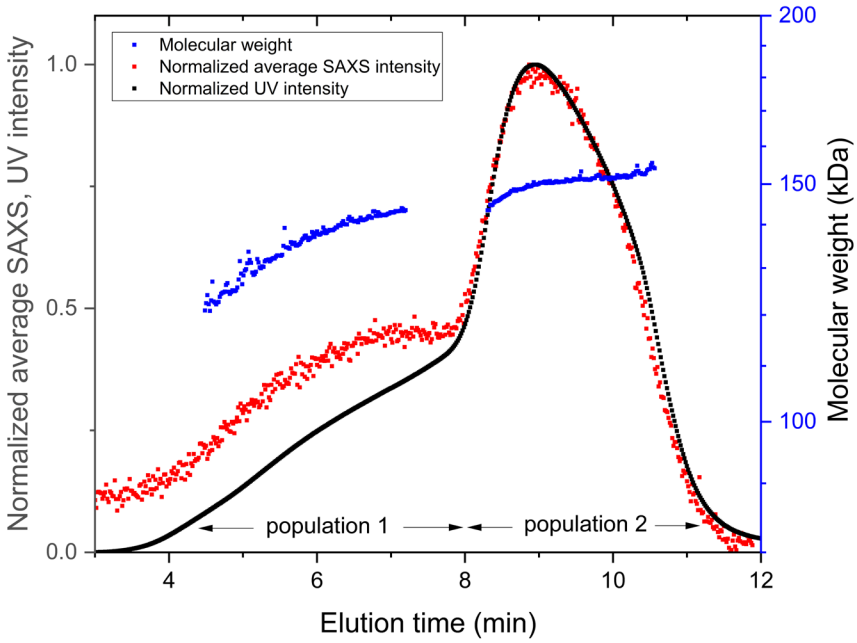

Fig. 12. Fractogram of mAb, 300 µg injected, with peak-maximum normalized average intensities of SAXS (red) and UV absorption at 280 nm (black) vs elution time. Overlayed molecular weight in log scale (blue), increasing from 120 kDa to approximately140 kDa in population 1 and approximately constant at 150 kDa over population 2

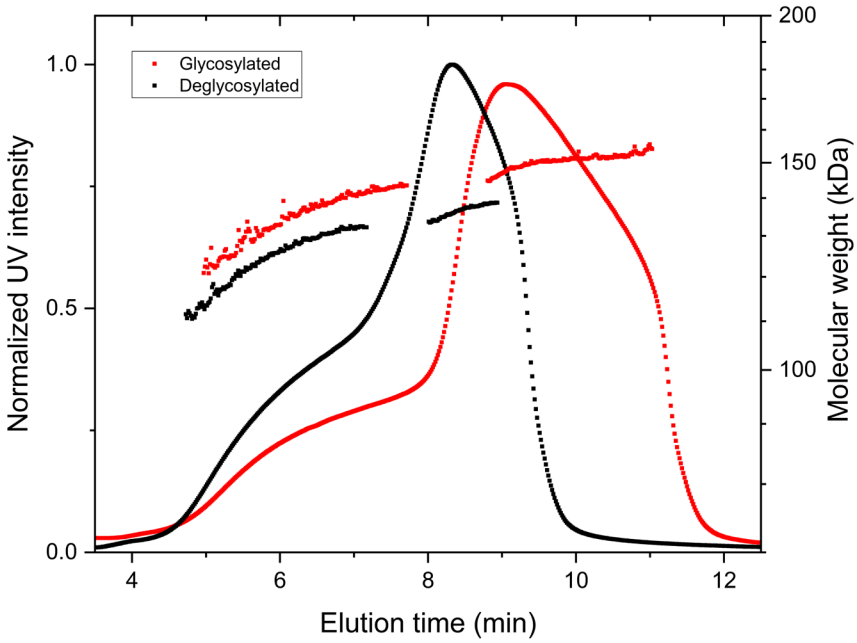

Fig. 13. UV (280) fractograms of glycosylated (red) and deglycosylated (black) mAb. Molecular weights follow the same color coding as the UV signal. Molecular weight in log scale, increasing from 110 kDa to approximately130 kDa for population 1 and approximately 135–140 kDa over population 2 for the deglycosylated sample. For the glycosylated sample molecular weights are 120–140 kDa over population 1 and 150 kDa for population 2.

After comparison between *P(r)* and Kratky plots from the two populations respectively, it could be concluded that the existence of two populations is a consequence of partial degradation of the molecule. In the *P(r)* (see figure 14) it was observed that the maximum distance between scattering centres inside the molecule, D_{max}, was higher for population 1. This means that an elongation occurs. From the Kratky plots (see figure 15), a higher flexibility of the population 1 molecule was observed. In conclusion, when the molecule degrades the degree of freedom increases and parts of the molecule are given room to extend into formerly excluded volumes, hence elongation and higher flexibility.

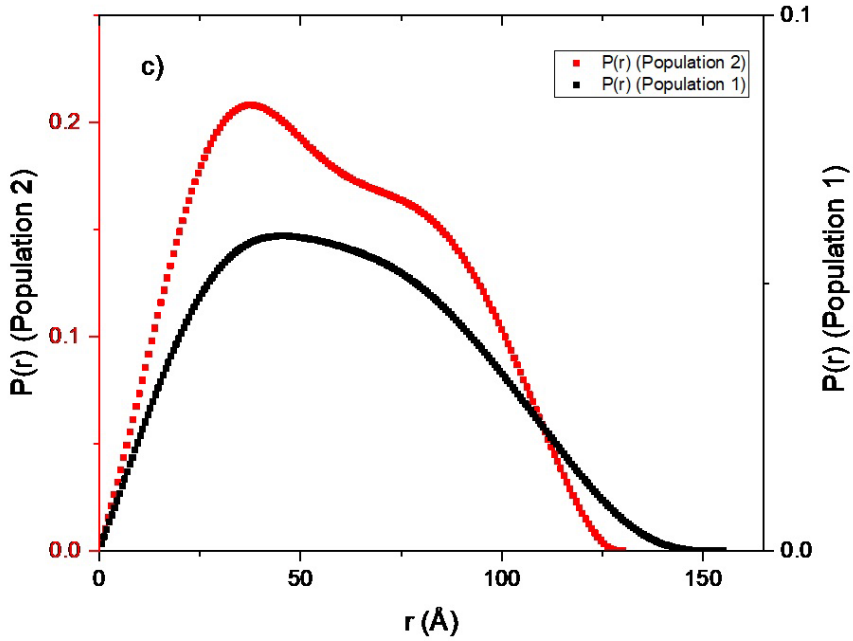

Fig. 14. *P(r)* functions of Trastuzumab populations 1 and 2 respectively. D_{max} is higher for population 1, indicating an elongation. The features indicating domains in population 2 are less pronounced in population 1.

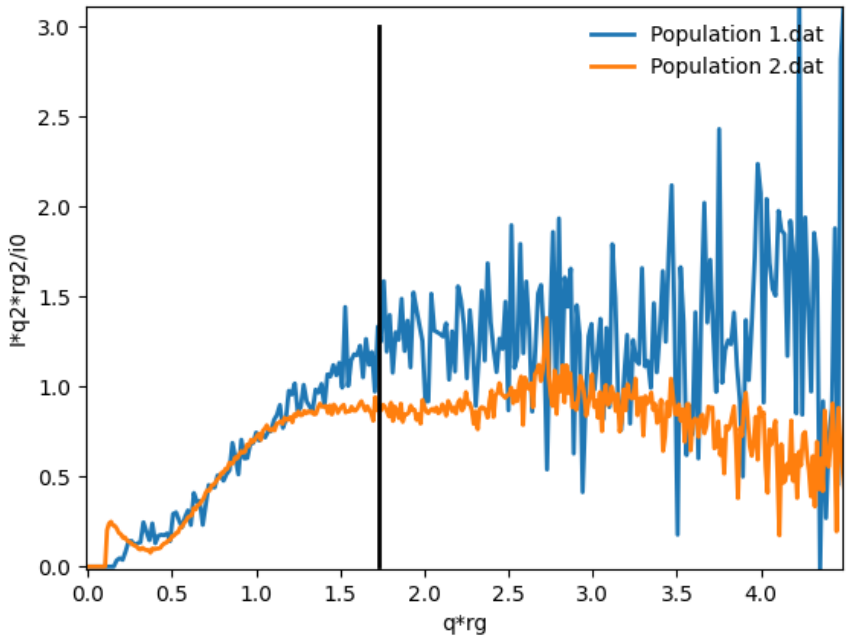

Fig. 15. q^2-Normalized Kratky plots for populations 1 (blue) and 2 (orange) respectively. The black line indicates $q^*R_g = \sqrt{3}$, where globular proteins have their maximum.

Looking forward

There is an increasing interest in the work concluded in this thesis and mainly for the AF4-SAXS coupling technique. Since this is a new way of characterizing soft matter in solution and its ability to closer to in-situ study sensitive sample systems with many components using SAXS, there is an interest in exploring the technique further. The exploratory work has already started and Casein micelles, Lipid nanoparticles (LNP), and nanoparticle interactions in plasma/serum are examples of applications which surely will show up continuously in literature (33). AF4 has in recent years shown an increasing rate of application areas and consequently publications within the pharmaceutical development community (22, 34-37). With the pandemic and a Nobel prize winner close in memory, it is believed that loaded (m-RNA, and other APIs) and unloaded LNPs can be characterized using the AF4-SAXS technique. Compared to other existing techniques, the gentle fractionation followed by SAXS of formulated LNPs may turn out to be a route for further learnings. It has also been shown lately (10, 38, 39) that AF4 can be used for the fractionation of API in blood to study the interaction with serum and plasma proteins.

Large-scale research facilities and their users dealing with small angle scattering (SAS) are also showing an increasing interest. It would not be surprising if this technique could also be applied to small angle neutron scattering (SANS). To realize the AF4-SANS coupling it would probably be necessary to work on elements with higher scattering length densities or systems with significant scattering length density differences, since the flux in neutron sources is magnitudes lower compared to synchrotron sources. Another option would be the utilization of stop flow; to guide a fraction into the SANS measuring cell where the flow is temporarily stopped.

NextBioForm has received extended funding to explore the AF4-UV-SAXS technique further. The first steps will be to explore possibilities and limitations and the applications will come in mainly from the pharmaceutical sphere of interest.

Acknowledgements

This part of thesis writing can easily become cringey to me (Thank you **Ida** for continuously updating my vocabulary), I decided to try and keep the cringe level low and of course without forgetting anyone important for the triumph of this examination. Let's see how it goes.

A thesis is not complete without a stunning cover, thank you **Amanda** and **Ebba** for your creative input.

The support given by **Marie** and **Lars** is what made the conclusion of this thesis possible. Thank you. Sometime after the start of my employment at Lund University I started to feel the need to have a bigger part in research. At the same time, I saw an opportunity to develop professionally and to keep my interest in learning alive. What better way, at a university, than to pursue doctoral studies. You may call me a late bloomer, but we are also important for the ecosystem.

Anyway, without the support from **Marie**… Marie, I am very grateful for your way of letting everyone bloom, not being afraid of professional development of a striving employee, but rather to encourage it for the better of all. Like you said, -Såhär, det är klart att du ska arbeta för att åtminstone göra en Lic. You formalized it by taking me in under the NextBioForm umbrella, solved the financing, and sped up the pace. You inspire great new things, and you are wise.

Thanks to NextBioForm for funding and for providing an inspiring environment to be part of.

Laze, worldclass researcher with a fantastic personality. The rare combination does not come flying in the wind. (Cringey, yes a little😊). Lars introduced me already from my start at Lund University to AF4 and has always been encouraging and open to cooperation. My feeling has always been that it's been for the benefit of my professional development, which is highly appreciated and of course a result of the way you conduct and communicate.

I would like to thank all colleagues at the department and my fellow NextBioForm PhD-students, Amanda, Anna-Maria, Daniel, Ingrid, Johanna, Lingping, Shuai, and Zandra. Thank you to all co-writers for your contributions, Andreas, Christopher, Fátima, Stephen, and Yi.

Special thanks to **Olexandr Fedkiv** for covering for me when not being present.

Thank you, **Jessica** (wife and the love of my life), for being my supporter, my best friend and in a way also my psychiatrist, and my mentor. Happy to share this experience with you.

References

1. Krumbein WC. A history of the principles and methods of mechanical analysis. Journal of Sedimentary Research. 1932;2(2):89-124.
2. Litzén A, Wahlund KG. Improved separation speed and efficiency for proteins, nucleic-acids and viruses in asymmetrical flow field flow fractionation. Journal of Chromatography. 1989;476:413-21.
3. Wahlund KG, Litzén A. Application of an asymmetrical field-flow fractionation channel to the separation and characterization of proteins, plasmids, plasmid fragments, polysaccharides and unicellular algae. Journal of Chromatography. 1989;461:73-87.
4. Litzén A, Walter JK, Krischollek H, Wahlund KG. Separation and quantitation of monoclonal-antibody aggregates by asymmetrical flow field-flow fractionation and comparsion to gel-permeation chromatography. Analytical Biochemistry. 1993;212(2):469-80.
5. Wahlund KG, Giddings JC. Properties of an asymmetrical flow field-flow fractionation channel having one permeable wall. Analytical Chemistry. 1987;59(9):1332-9.
6. Litzen A, Wahlund KG. Zone broadening and dilution in rectangular and trapezoidal asymmetrical flow field-flow fractionation channels. Analytical Chemistry. 1991;63(10):1001-7.
7. Osorio-Macías DE, Bolinsson H, Linares-Pastén JA, Ferrer-Gallego R, Choi J, Peñarrieta JM, et al. Characterization on the impact of different clarifiers on the white wine colloids using Asymmetrical Flow Field-Flow Fractionation. Food Chem. 2022;381.
8. Bian J, Gobalasingham N, Purchel A, Lin J. The Power of Field-Flow Fractionation in Characterization of Nanoparticles in Drug Delivery. Molecules. 2023;28(10).
9. Chen X, Zhang WH, Dou YW, Song TG, Shen SG, Dou HY. Applications of asymmetrical flow field-flow fractionation for separation and characterization of polysaccharides: A review. Journal of Chromatography A. 2021;1635.
10. Leeman M, Nilsson AC, Nilsson L. Analysis of Proteins, Biologics, and Nanoparticles in Biological Fluids Using Asymmetrical Flow Field-Flow Fractionation. Lc Gc Europe. 2022;35(1):7-13.
11. Malik MI, Pasch H. Field-flow fractionation: New and exciting perspectives in polymer analysis. Progress in Polymer Science. 2016;63:42-85.

12. Nilsson L. Separation and characterization of food macromolecules using field-flow fractionation: A review. Food Hydrocolloids. 2013;30(1):1-11.
13. Ventouri IK, Loeber S, Somsen GW, Schoenmakers PJ, Astefanei A. Field-flow fractionation for molecular-interaction studies of labile and complex systems: A critical review. Anal Chim Acta. 2022;1193.
14. Bolinsson H, Lu Y, Hall S, Nilsson L, Håkansson A. An alternative method for calibration of flow field flow fractionation channels for hydrodynamic radius determination: The nanoemulsion method (featuring multi angle light scattering). Journal of Chromatography A. 2018;1533:155-63.
15. Bolinsson H, Söderberg C, Herranz-Trillo F, Wahlgren M, Nilsson L. Realizing the AF4-UV-SAXS on-line coupling on protein and antibodies using high flux synchrotron radiation at the CoSAXS beamline, MAX IV. Anal Bioanal Chem. 2023;415(25):6237-46.
16. Plivelic TS, Terry AE, Appio R, Theodor K, Klementiev K, editors. X-Ray Tracing, Design and Construction of an Optimized Optics Scheme for CoSAXS, the Small Angle X-ray Scattering beam line at MAX IV Laboratory. 13th International Conference on Synchrotron Radiation Instrumentation (SRI); 2018 Jun 10-15; Natl Synchrotron Radiat Res Ctr, Taipei, TAIWAN2019.
17. Wahlund KG. Flow field-flow fractionation: Critical overview. Journal of Chromatography A. 2013;1287:97-112.
18. Giddings JC, Chen XR, Wahlund KG, Myers MN. Fast particle separation by flow steric field-flow fractionation. Analytical Chemistry. 1987;59(15):1957-62.
19. Wahlund KG, Nilsson L. Flow FFF – Basics and Key Applications. In: Williams SKR, Caldwell K, editors. Field-Flow Fractionation in Biopolymer Analysis. Wien: Springer; 2012. p. 1-305.
20. Giddings JC, Yang FJF, Myers MN. Flow field-flow fractionation - versatile new separation method. Science. 1976;193(4259):1244-5.
21. Giddings JC, Yang FJ, Myers MN. Theoretical and experimental characterization of flow field-flow fractionation. Analytical Chemistry. 1976;48(8):1126-32.
22. Västberg A, Bolinsson H, Leeman M, Nilsson L, Nylander T, Sejwal K, et al. Investigating thermally induced aggregation of Somatropin- new insights using orthogonal techniques. Int J Pharm. 2023;637.
23. Einstein A. A new determination of the molecular dimensions. Annalen Der Physik. 1906;19(2):289-306.
24. Håkansson A, Magnusson E, Bergenståhl B, Nilsson L. Hydrodynamic radius determination with asymmetrical flow field-flow fractionation using decaying cross-flows. Part I. A theoretical approach. Journal of Chromatography A. 2012;1253:120-6.
25. Magnusson E, Håkansson A, Janiak J, Bergenståhl B, Nilsson L. Hydrodynamic radius determination with asymmetrical flow field-flow fractionation using decaying cross-flows. Part II. Experimental evaluation. Journal of Chromatography A. 2012;1253:127-33.

26. Häusele B, Gindele MB, Cölfen H. Revision of the calibration experiment in asymmetrical flow field-flow fractionation. Journal of Chromatography A. 2021;1635:461631.
27. Guinier A, Fournet G. Small-angle scattering of X-rays: John Wiley & Sons, Inc.; 1955.
28. Glatter O, Kratky O. Small Angle X-ray Scattering: Academic Press; 1982.
29. F.R.S LR. On the electromagnetic theory of light. Philosophical Magazine. 1881;Series 5:12:73.
30. Zielke C, Stradner A, Nilsson L. Characterization of cereal β-glucan extracts: Conformation and structural aspects. Food Hydrocolloids. 2018;79:218-27.
31. Guinier A. The diffusion of x-rays under the extremely weak angles applied to the study of fine particles and colloidal suspension. Comptes Rendus Hebdomadaires Des Seances De L Academie Des Sciences. 1938;206:1374-6.
32. Kratky O, Porod G. Diffuse small-angle scattering of X-rays in colloid systems. Journal of Colloid Science. 1949;4(1):35-70.
33. Graewert MA, Wilhelmy C, Bacic T, Schumacher J, Blanchet C, Meier F, et al. Quantitative size-resolved characterization of mRNA nanoparticles by in-line coupling of asymmetrical-flow field-flow fractionation with small angle X-ray scattering. Scientific Reports. 2023;13(1).
34. Hawe A, Romeijn S, Filipe V, Jiskoot W. Asymmetrical flow field-flow fractionation method for the analysis of submicron protein aggregates. Journal of Pharmaceutical Sciences. 2012;101(11):4129-39.
35. Hinna A, Steiniger F, Hupfeld S, Brandl M, Kuntsche J. Asymmetrical flow field-flow fractionation with on-line detection for drug transfer studies: a feasibility study. Anal Bioanal Chem. 2014;406(30):7827-39.
36. Lohrke J, Briel A, Mäder K. Characterization of superparamagnetic iron oxide nanoparticles by asymmetrical flow-field-flow-fractionation. Nanomedicine. 2008;3(4):437-52.
37. Gidlöf Z, Pedersen BL, Nilsson L, Teleman A, Wahlgren M, Millqvist-Fureby A. Utilising phase diagram to understand barley starch microsphere preparation in an aqueous two-phase system. Colloids and Surfaces a-Physicochemical and Engineering Aspects. 2023;658.
38. Ramm I, Leeman M, Schagerlöf H, Leon IR, Castro A, Nilsson L. Investigation of native and aggregated therapeutic proteins in human plasma with asymmetrical flow field-flow fractionation and mass spectrometry. Anal Bioanal Chem. 2022;414(29-30):8191-200.
39. Leeman M, Choi J, Hansson S, Storm MU, Nilsson L. Proteins and antibodies in serum, plasma, and whole blood-size characterization using asymmetrical flow field-flow fractionation (AF4). Anal Bioanal Chem. 2018;410(20):4867-73.

Printed by Media-Tryck, Lund 2024 NORDIC SWAN ECOLABEL 3041 0903

LUND UNIVERSITY

Faculty of Engineering
Department of Process and
Life Science Engineering
Division of Food and Pharma
ISBN 978-91-8096-054-0